

Research Paper

Tissue Distribution of Indinavir Administered as Solid Lipid Nanocapsule Formulation in *mdr1a* (+/+) and *mdr1a* (-/-) CF-1 Mice

Manuela Pereira de Oliveira,¹ Emmanuel Garcion,² Nicolas Venisse,^{1,3} Jean-Pierre Benoît,² William Couet,^{1,3} and Jean-Christophe Olivier^{1,4}

Received May 14, 2005; accepted May 14, 2005

Purpose. Due to protease inhibitor (PI) efflux transport by P-glycoprotein (P-gp), insufficient PI concentrations result in low ongoing HIV replication in the so-called virus sanctuaries (brain and testes). The aim of the present study was to evaluate indinavir-loaded nanocapsules (Ind-LNC) including Solutol[®] HS15, an excipient reported to possess *in vitro* P-gp inhibiting properties, as a means to improve indinavir distribution into brain and testes of mice.

Methods. Normal *mdr1a* (+/+) or P-gp-deficient *mdr1a* (-/-) CF-1 mice were dosed with Ind-LNC (10 mg indinavir/kg, i.v.). At 30 min postadministration, indinavir was determined in plasma, brain, testes, as well as in kidneys, liver, and heart by LC-MS/MS, and tissue/plasma concentration ratios were calculated. Results were compared with those of control groups that received an indinavir solution (Ind-Sol).

Results. Using Ind-Sol, ratios were 21.3- and 3.3-fold higher in brains and testes of *mdr1a* (-/-) mice than of *mdr1a* (+/+) mice, respectively, whereas in the other organs ratios were not significantly different between the two substrains. When Ind-LNC was used, a similar [*mdr1a* (-/-) vs. *mdr1a* (+/+) mice] trend was observed. Moreover, ratios were found to be significantly increased (1.9-fold increase in average) in most organs (brain and testes in particular) with Ind-LNC compared to Ind-Sol, regardless of the substrain used.

Conclusions. In agreement with previous works, P-gp governs at least in part indinavir uptake into brain and testes. LNC formulation increased indinavir uptake in brain and testes by mechanisms other than, or additional to, P-gp inhibition.

KEY WORDS: CF-1 mice; indinavir; P-glycoprotein; solid lipid nanocapsule; Solutol[®] HS15.

INTRODUCTION

Inhibitors of HIV-1 protease, such as indinavir, comprise a major advance in the clinical management of HIV-1 infection. Their use in combination with HIV-1 reverse transcriptase inhibitors leads to a dramatic reduction of plasma viremia in patients (1). However, ongoing low active replication of the virus occurs in viral “sanctuaries” such as brain and testes (2,3), leading to neurologic disorders (AIDS dementia complex) (4), to the persistence of sexual transmission of the infection (5), and to the selection of resistant mutants (6).

A common characteristic of blood–brain (BBB) and blood–testis barriers is the presence of the adenosine triphosphate (ATP)-dependent drug efflux pump P-glycoprotein (P-gp), which transports a wide range of compounds of unrelated chemical structures (7,8). P-gp is encoded by the *MDR1* gene in humans and the *mdr1a* and *mdr1b* genes in mice and rats. Although P-gp functions are not fully elucidated, one of its major roles is probably to prevent the uptake of toxic xenobiotics (9,10). Thus, P-gp expression at the blood–brain and blood–testis barriers has been shown to reduce the entry of protease inhibitors (PI), indinavir included, into the brain parenchyma and the seminal plasma (11–13).

Colloidal drug carrier systems hold the promise of overcoming physiological barriers to promote a successful therapy (14,15). Recently, novel solid lipid nanocapsules (LNC), composed of a liquid lipid core (medium chain triglycerides) surrounded by a solid surfactant shell (Solutol[®] HS15 and lecithin), were developed as drug carriers (16). Radiolabeled LNC, intravenously administered to rats, presented a prolonged half disappearance time (around 45 min) attributed to the presence of polyethylene glycol 660 at the nanocapsule surface and mainly accumulated in liver (17). Solutol[®] HS15—a mixture of polyethyleneglycol 660 mono- and

¹Faculté de Médecine & Pharmacie, EA3809 “Pharmacologie des Médicaments Anti-Infectieux”, Pôle Biologie-Santé, 40 av. du Recteur Pineau, 86022 Poitiers CEDEX, France.

²Inserm-U 646 Bâtiment IBT, 10 rue André Boquet, 49100 Angers, France.

³Faculté de Médecine & Pharmacie, Laboratoire de Pharmacocinétique, Centre Hospitalo-Universitaire de Poitiers, Pôle Biologie-Santé, 86022 Poitiers CEDEX, France.

⁴To whom correspondence should be addressed. (e-mail: jean.christophe.olivier@univ.poitiers.fr)

ABBREVIATIONS: Ind-LNC, indinavir-loaded lipid nanocapsules; Ind-Sol, indinavir solution; LNC, lipid nanocapsule.

diesters of 12-hydroxystearate, and of about 30% (m/m) polyethyleneglycol 660 (BASF Technical Bulletin, 2004) included in LNC formulations—was reported to be an inhibitor of P-gp (18,19) and of cytochrome P450 3A4 (20). The aim of this study was to compare the distribution of indinavir formulated as a solution (Ind-Sol) or as solid lipid nanocapsules (Ind-LNC) in tissues isolated by blood–tissue barriers (brain and testes) and in other tissues (kidneys, liver, and heart) in normal or P-gp-deficient CF-1 mice to evaluate the benefit of formulating indinavir as nanocapsules including a P-gp inhibitor.

MATERIALS AND METHODS

Materials

Indinavir was extracted from Crixivan[®] (Merck) tablets as previously described (21). Amprenavir was kindly provided by GlaxoSmithKline (GSK, Hertfordshire, UK). The lipophilic Labrafac[®] WL 1349 (caprylic acid triglycerides) was kindly provided by Gattefossé (Saint-Priest, France). Lipoid[®] S75-3 (soybean lecithin at 69% of phosphatidylcholine) and Solutol[®] HS15 were kindly provided by Lipoid (Ludwigshafen, Germany) and BASF (Ludwigshafen, Germany), respectively. Because of their complex compositions, the brand names of these excipients will be used throughout the text. Cholesterol was purchased from Sigma (St Quentin-Fallavier, France). Solvents were of HPLC grade and all other chemicals were of analytical grade. Highly purified water was produced by a MilliQ gradient[®] Plus Millipore system (St Quentin-en-Yvelines, France). Analysis Oasis MCX Solid Phase Extraction (SPE) cartridges were supplied by Waters (St Quentin-en-Yvelines, France).

Animals

Animals in this study were handled in accordance with the provisions of the “Principles of Laboratory Animal Care” (NIH publication # 85-23, revised 1985). Male and female CF-1 mice [*mdr1a* (+/+) and *mdr1a* (-/-)] were obtained from Charles Rivers Laboratories (Wilmington, MA, USA) and were maintained in the animal unit. Adult male mice (29 ± 2 g, 10 weeks old) used for the study were housed in a light–(12-h light/dark cycle) and temperature-controlled environment for at least 5 days before experiments, with free access to water and food. Food was withdrawn 12 h before the experiments.

LNC Preparation

LNC preparation was based on a phase inversion process involving two steps (16). Step I consisted of magnetic stirring of all components: indinavir (0.017 g first solubilized in ethanol (0.10 g) and dichloromethane (0.075 g), cholesterol (0.04 g), Labrafac[®] WL 1349 (1.2 g), Lipoid[®] S75-3 (0.07 g), Solutol[®] HS15 (1.5 g), NaCl (0.02 g), and water (1.5 g). Temperature was raised to 85°C and gradually cooled down to 60°C. Three temperature cycles were applied until final cooling to 70°C. Step II was an irreversible thermal shock induced by adding 3 mL of cold water at about 0°C, which led to the formation of nanocapsules. Afterwards, slow magnetic

stirring was applied to the suspension for 5 min in an ice bath. LNC were immediately used for experiments.

LNC Size Measurements

The average volume diameters of nanoparticles were determined at 25°C by photon correlation spectroscopy using a Malvern Autosizer 4700 (Malvern Instruments, Worcester-shire, UK) fitted with a 188-nm laser beam at a fixed angle (90°).

LNC Entrapment Efficiency

To evaluate entrapment efficiency, 2 mL of Ind-LNC were added to a MicroSep 3 K Omega filter (Pall Corporation, St Germain-en-Laye, France). After centrifugation at 4,000 g for 45 min, indinavir concentrations of filtrates (untrapped indinavir) were determined by LC-MS/MS, and entrapment efficiency was deduced considering a filtration recovery of 100% as determined with a control 2 mmol/L indinavir solution (i.e., Ind-Sol). LNC loading was calculated by dividing the amount of entrapped indinavir by the amount of LNC excipients.

Indinavir Solutions

For intravenous administrations, indinavir solutions (Ind-Sol; 2 mmol/L) were prepared in 0.9% (m/v) saline containing 10% ethanol, adjusted to pH 3 with 1 mol/L HCl. This acidic solution was shown *in vitro* to be neutralized by mice blood according to the ratio 100 µL drug solution/1 mL mice blood.

Tissue Distribution Experiment

Ind-Sol or Ind-LNC was administered to mice as a bolus (10 mg/kg, *n* = 6) via the caudal vein. The mean injection volume was 233 ± 15 µL, which corresponded to a drug formulation/blood volume ratio of 100 µL:1 mL, considering a blood volume of 1.7 mL per 0.020 kg body weight (22). *In vitro* experiments showed that at this ratio blood buffering capacities efficiently neutralized the acidic Ind-Sol formulation (data not shown). Tissue samples were collected at a postequilibrium distribution time, i.e., 30 min postadministration, as determined in preliminary experiments showing no significant differences between tissue/plasma ratios obtained at 10 or 30 min postadministration (data not shown). Just before blood collection mice were anaesthetized with isofluran (Forene[®]; Abbott, Rungis, France) inhalation in airtight enclosure supplied with air–isofluran mixture (3.7%) at a flow of 500 mL/min (Anaesthesia Unity, Univentor 400; Phymep, Paris, France). Blood samples were collected by cardiac puncture. Animals were immediately sacrificed; brain, testes, kidneys, liver, and heart were collected and rinsed with 0.9% (m/v) saline. Plasma and tissues were stored at –20°C until LC-MS/MS analysis.

Plasma Sample Preparation

Indinavir was determined after extraction from plasma as previously described (23,24). Fifty microliters of a 10

mol/L amprenavir internal standard solution, 50 μL of a 5 mol/L sodium hydroxide solution, 50 μL methanol, and 1 mL ethyl acetate were added to 50 μL thawed plasma and shaken for 30 s. After centrifugation (10 min, 3,000 g), organic layers were collected and evaporated under nitrogen at 40°C. Residues were redissolved in 100 μL of mobile phase for LC-MS/MS analysis.

Tissue Sample Preparation

For indinavir extraction from tissues, 125 μL of 0.9% (m/v) saline, 50 μL of a 10 $\mu\text{mol/L}$ amprenavir internal standard solution, and 1 mL of 0.1 mol/L HCl were added to thawed samples (250 mg for brain or 100 mg for other organs). After grinding for 2 min, samples were centrifuged for 10 min at 3,000 g. Supernates were collected and submitted to an additional centrifugation for 5 min at 12,500 g. Resulting supernates were further transferred onto SPE cartridges conditioned with 1 mL methanol followed by 1 mL water. Cartridges were then successively washed with 1 mL of 0.1 mol/L HCl, 1 mL methanol, and 1 mL of a 5% methanol–2% ammonium hydroxide aqueous solution. Analytes were finally eluted with 1 mL of a 95% methanol–2% ammonium hydroxide aqueous solution. After evaporation under nitrogen at 40°C, residues were redissolved in 100 μL of mobile phase for LC-MS/MS analysis.

LC-MS/MS Procedure

The procedure was adapted from an LC-MS/MS method used to quantify indinavir in plasma samples (25).

Apparatus

Detection was performed with a Micromass[®] Quattro micro API a high-performance quadrupole mass spectrometer (Waters). Waters Alliance separations module 2695 constituted the pump and the injector. Quantitative and qualitative analyses were performed using Masslynx[®] version 4.0 software Waters.

MS–MS parameters

Mass spectral analyses were accomplished in the positive ion mode. Tuning parameters were individually optimized for each drug to obtain the best signal/noise (S/N) ratio for indinavir and amprenavir. Mass spectral transitions, monitored for indinavir and amprenavir, were 614.14/421.30 and 506.09/245.30 (*m/z*), respectively.

Liquid Chromatography Parameters

The column was a Nucleosil 100-5C18 (5 μm , 150 \times 1 mm i.d.; Macherey-Nagel, Hoerdt, France). A linear gradient was used to separate compounds, with a 10 mmol/L ammonium formate aqueous solution, adjusted to pH 4.1 with formic acid, as solvent A and a 0.1% v/v solution of formic acid in acetonitrile as solvent B. The two components of mobile phase were filtered and degassed under vacuum. The flow rate was 0.1 mL/min and the injection volume was 10 μL . At each analysis the A/B ratio initially set at 55:65 v/v

linearly ramped to 65:55 over 5 min and returned to 55:65 over 0.1 min. This condition was held for 5 min prior to the injection of the next sample. The brain calibration curves were linear from 0.0012 (LOQ) to 0.038 $\mu\text{mol/kg}$. The testis, kidney, liver, and heart calibration curves were linear from 0.39 to 12.5 $\mu\text{mol/kg}$.

Western Blot

Tissues were homogenized on ice with a mechanical dounce in 1.5 mL of lysis buffer containing protease inhibitors (50 mM Tris–HCl, 5 mM EDTA, 150 mM NaCl, 1% Triton[®] X-100, 2 mM phenylmethylsulfonyl fluoride, 1 $\mu\text{g/mL}$ pepstatin A, 2 $\mu\text{g/mL}$ aprotinin, 5 $\mu\text{g/mL}$ leupeptin, pH 7.4). Homogenized samples were then left on ice for 30 min. Soluble extracts were further collected and separated from insoluble debris by centrifugation at 12,000 g for 10 min at 4°C. The insoluble pellets were washed once with lysis buffer and solubilized in a small volume of solubilization buffer [50 mM Tris–HCl, 5 mM EDTA, 1% sodium dodecylsulfate (SDS)] by passage through a 21-gauge needle and diluted in lysis buffer to the same volume as the supernatants. Supernatants were also adjusted to an SDS concentration equal to that of the solubilized pellets. The amount of total soluble protein in the extracts was determined with the Bio-Rad detergent-compatible protein assay with bovine serum albumin (BSA) as standard. For Western blotting, 20 μg of total proteins for each sample were then separated by SDS–PAGE and electroblotted onto nitrocellulose membranes (Hybond-P; Amersham Bioscience Europe, Orsay, France). Membranes were blocked in 4% BSA in Tris-buffered saline (TBS) for 1 h at room temperature. Blots were incubated with primary antibody overnight (C219 at 1/80 dilution; Clinisciences, Montrouge, France) at 4°C in 4% BSA in TBS containing 0.1% Tween 20 (TBS-T), followed by a 2-h incubation with the appropriate antimouse secondary peroxidase-conjugated antibody (Amersham) in TBS-T. The immunoreactive proteins were visualized using diaminobenzidine in TBS added with 0.03% H_2O_2 and qualitative comparisons were carried out.

Statistical Analysis

Tissue distribution data were compared by Student's *t* test or by Mann–Whitney *U* test. The level of significance was set at $P < 0.05$.

RESULTS

Nanoparticle Characterization

The average volume diameter of indinavir-loaded LNC was 38 ± 0.1 nm ($n = 3$). Entrapment efficiency was found to be $50 \pm 0.6\%$ ($n = 3$) of the initial indinavir amount, which corresponded to 1.9 ± 0.1 nmol per mg nanoparticle excipient, the balance being probably solubilized within polyethyleneglycol 660 12-hydroxy-stearate micelles. A fraction of the newly formulated LNC may be less stable as a result of slightly reduced amounts of internalized lecithin, which likely represents the LNC frame. Thus the filtration used to separate free indinavir from indinavir entrapped in

LNC is susceptible to break those more fragile objects and underestimates initial indinavir entrapment efficiency.

P-gp Expression

Results of Western blot analysis of P-gp expression in the two mouse substrains are shown in Fig. 1. The *mdr1a* (+/+) CF-1 mice showed intense banding of the P-gp in heart, liver, and testes and slightly lower expression levels in brain and kidneys. In addition, *mdr1a* (-/-) CF-1 mice used in the present study have nondetectable (brain, liver, and heart) or very low (kidneys and testes) levels of P-gp expression.

In Vivo Distribution of Indinavir

Indinavir concentrations in tissues and plasma are presented in Table I. To facilitate tissue uptake comparisons, tissue concentrations were corrected from plasma fluctuation by calculating tissue/plasma concentration ratios (Table I). Relative variations and statistical comparisons of tissue/plasma concentration ratios are presented in Table II.

Plasma and Tissue Concentrations

After the administration of Ind-Sol to *mdr1a* (+/+) mice, the lowest concentrations were found in brain and testes, and the highest levels in liver and kidneys (Table I). Significantly higher indinavir concentrations were determined in brain and testes of *mdr1a* (-/-) mice compared to *mdr1a* (+/+) mice, whereas the converse was observed in liver and kidneys. However, plasma and heart concentrations were not significantly different between the two mouse substrains. Using the Ind-LNC formulation, a two times higher concentration was observed in plasmas of *mdr1a* (+/+) mice compared to plasmas of *mdr1a* (-/-) mice. Regardless of the mouse substrain used, higher concentrations were generally observed in tissues of mice injected with LNC formulation compared to mice treated with indinavir solution. Significant increases in indinavir concentrations were observed in brain and testes of *mdr1a* (-/-) mice compared to *mdr1a* (+/+) mice.

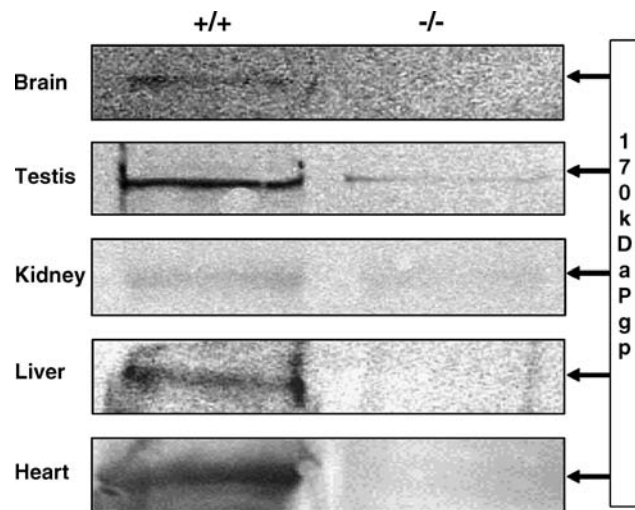


Fig. 1. Western blot analysis of P-gp in tissues collected from *mdr1a* (+/+) and *mdr1a* (-/-) CF-1 mice.

Table I. Tissue, Plasma Concentrations, and Tissue/Plasma (*t/p*) Ratios of Indinavir, 30 min After Ind-Sol or Ind-LNC Intravenous Administration to *mdr1a* (+/+) and (-/-) CF-1 Mice (10 mg/kg), *n* = 6 (Means ± SD)

Tissues	Ind-Sol		Ind-LNC	
	<i>mdr1a</i> (+/+) concentration (μmol/kg)	<i>mdr1a</i> (-/-) concentration (μmol/kg)	<i>mdr1a</i> (+/+) concentration (μmol/kg)	<i>mdr1a</i> (-/-) concentration (μmol/kg)
Brain	0.046 ± 0.023*	0.804 ± 0.166*	0.099 ± 0.055*	0.877 ± 0.156*
Testes	0.371 ± 0.112*	0.995 ± 0.062*	0.664 ± 0.163*	1.052 ± 0.173*
Kidneys	4.169 ± 2.050*	2.624 ± 0.304*	7.733 ± 2.159*	4.435 ± 0.746*
Liver	2.077 ± 1.125	1.229 ± 0.164	4.756 ± 0.916*	1.881 ± 0.564*
Heart	0.573 ± 0.283	0.521 ± 0.129	1.280 ± 0.349*	0.738 ± 0.209*
Plasma (μmol/L)	0.763 ± 0.411	0.631 ± 0.275	0.825 ± 0.351*	0.421 ± 0.083*
		<i>t/p</i> ratios	<i>t/p</i> ratios	<i>t/p</i> ratios
		0.066 ± 0.024	1.408 ± 0.461	0.123 ± 0.052
		0.553 ± 0.210	1.810 ± 0.666	0.859 ± 0.185
		5.793 ± 1.469	4.697 ± 1.604	10.19 ± 3.680
		2.867 ± 1.237	2.204 ± 0.811	6.286 ± 1.756
		0.780 ± 0.151	0.884 ± 0.186	1.333 ± 0.679
		-	-	-

* Statistically different (*p* < 0.05). Statistical comparisons of *t/p* ratios are presented in Table II.

Table II. Relative Variations with Statistical Comparisons of the Tissue/Plasma Indinavir Concentration Ratios Determined 30 min After i.v. Administration of Ind-Sol or Ind-LNC to *mdr1a* (+/+) or *mdr1a* (-/-) CF-1 Mice (10 mg/kg)

Tissues	<i>mdr1a</i> (-/-) vs. <i>mdr1a</i> (+/+) mice substrain comparisons		Ind-Sol vs. Ind-LNC comparisons	
	Ind-Sol	Ind-LNC	<i>mdr1a</i> (+/+) mice	<i>mdr1a</i> (-/-) mice
Brain	21.3*	17.3*	1.9*	1.5*
Testes	3.3*	3.0*	1.6*	1.4
Kidneys	0.8	1.1	1.8*	2.3*
Liver	0.8	0.7	2.2*	2.1*
Heart	1.1	1.7	1.7	2.0*

* Statistically different ($p < 0.05$).

mice, whereas the converse was observed in liver, kidneys, and heart.

Effect of P-gp Deficiency on Indinavir Organ Uptake

In *mdr1a* (+/+) mice treated with Ind-Sol, tissue/plasma concentration ratios were much higher in kidneys and liver than in heart, testes, and brain (Tables I and II). The lowest ratios were observed in brains. In *mdr1a* (-/-) mice, as a result of the increase in indinavir tissue concentrations, tissue/plasma ratios determined in brain and testes were found to be 21.3- and 3.3-fold higher, respectively, compared to *mdr1a* (+/+) mice (both increases were significant). Tissue/plasma ratios determined in heart, kidneys, and liver were not significantly different between the two mouse substrains. Similar observations were made after the administration of Ind-LNC formulation (Tables I and II).

Effect of the Formulation on Indinavir Organ Uptake

In both substrains, tissue/plasma ratios were in general significantly higher (with increase factors ranging from 1.4 to 2.3 times) in all organs tested after the administration of Ind-LNC compared to Ind-Sol (Table II).

DISCUSSION

In mice, the efflux transporter P-gp responsible for multidrug resistance is encoded by two genes, *mdr1a* and *mdr1b*, the relative expressions of which are generally tissue-dependent (26). In *mdr1a* (+/+) CF-1 mice used in this study, P-gp was detected in heart, brain, testes, kidneys, and liver (Fig. 1). The lower P-gp expression observed in brain and kidneys was ascribed to the low relative number of cells expressing P-gp in these organs (e.g., mainly endothelial cells and astrocytes in brain, and epithelial cells in kidneys). In P-gp-deficient subpopulations of CF-1 mice, only P-gp derived from the *mdr1a* gene is lacking. The *mdr1a* genes of these mice have indeed an insertion of approximately 8.35 kb of a murine leukemia virus DNA at the exon 23 intron-exon junction resulting in the aberrant splicing of the mRNA and the loss of exon 23 during RNA processing (27). Although compensatory mechanisms involving an upregulation of the expression of the *mdr1b* gene products

have been reported (28), *mdr1a* (-/-) CF-1 mice used in this work have nondetectable levels of P-gp expression in brain, liver, and heart (Fig. 1), in agreement with results from previous works (29). P-gp found in testis and kidney tissues was attributed to the *mdr1b* gene expression (30).

To evaluate the impact of P-gp deficiency and of LNC formulation onto indinavir distribution, the concentrations of this P-gp substrate were determined in five organs (Table I) at a postdistribution equilibrium time point: brain and testes, separated from blood by physiological barriers with high P-gp efflux activity; heart, characterized by a high P-gp expression in cardiomyocytes; liver and kidneys, the P-gp of which is responsible for the excretion of xenobiotics into bile and urine, respectively (31). As mean plasma concentrations varied between groups (although nonsignificantly), tissue/plasma concentration ratios were calculated to allow comparisons of organ uptakes (Table I) and statistical comparisons presented in Table II.

In *mdr1a* (+/+) mice, the distribution of Ind-sol administered intravenously confirmed the poor penetration of this protease inhibitor into organs with blood-tissue barriers (brain and testes) compared to organs without barrier (kidneys, liver, and heart) (Tables I and II). As observed previously in P-gp-deficient transgenic mice (11,12,32), indinavir brain/plasma ratios were considerably increased in *mdr1a* (-/-) CF-1 mice compared to *mdr1a* (+/+) CF-1 mice (21.3-fold increase), confirming the high impact of P-gp-mediated efflux on indinavir distribution into brain tissue (11,12). P-gp deficiency also had a significant impact on indinavir distribution into testes, as shown by the significantly higher indinavir blood/testis concentration ratios in *mdr1a* (-/-) CF-1 mice compared to *mdr1a* (+/+) CF-1 mice (3.3-fold increase, Table II). The blood-testis barrier is more permeable than the BBB (33), which is confirmed in our study: despite a higher expression of P-gp in testis than in brain tissues of *mdr1a* (+/+) CF-1 mice (Fig. 1), indinavir uptake was higher in testes than in brain (Tables I and II). In testes of *mdr1a* (-/-) CF-1 mice, the residual P-gp was therefore in insufficient amount to maintain the functionality of the drug efflux. It is worth noting that tissue/plasma ratios determined in testes and brain of *mdr1a* (-/-) mice were higher than the levels determined in heart (Table II). Therefore, P-gp deficiency had apparently no impact on indinavir heart uptake despite the high P-gp expression level found in heart of *mdr1a* (+/+) CF-1 mice (Fig. 1). This result, in agreement with previous works by Kim *et al.* (11), contrasted with observations made on doxorubicin, a P-gp drug substrate shown to accumulate in hearts of *mdr1a* (-/-) knockout mice (34). Such a discrepancy may be explained by a lower recognition of indinavir than of doxorubicin by heart P-gp. Indeed, expression of P-gp is not the only limiting factor for substrate exclusion. For instance, P-gp association with tissue-specific proteins such as caveolins can modulate both P-gp oligomerization and affinities for substrates (35). Alternatively, redundant or compensatory mechanisms, exemplified by the expression of the mrp2 ABC-binding cassette transporter, of which indinavir is a substrate, may specifically correct for the loss of *mdr1a* gene in heart to maintain a partially functional efflux transport between blood and cardiomyocytes (36,37). High indinavir concentrations and tissue/plasma ratios were observed for kidneys and livers

of both mouse substrains, two organs that are known to excrete indinavir (31). The apparently lower uptake of indinavir by kidneys and livers of *mdr1a* (-/-) mice compared to *mdr1a* (+/+) mice being not statistically significant, P-gp deficiency does not seem to exert a significant impact on indinavir uptake and/or excretion by these organs.

To evaluate the effect of formulations on indinavir uptake in the five organs of interest, tissue/plasma ratios obtained after the administration of Ind-LNC were compared to ratios determined after the administration of Ind-Sol (Table II). In both mouse substrains, the LNC formulation induced similar increases of tissue-to-plasma ratios in all the organs (from 1.4 to 2.3 times) compared to indinavir solution, thus apparently independently of P-gp expression levels. Therefore, the P-gp-inhibiting effect of Solutol[®] HS15, which was demonstrated *in vitro* (18,38), had no significant impact on indinavir distribution *in vivo* when this excipient was included into LNC formulations for intravenous use. *In vitro* biological effects of Solutol[®] HS15 were generally observed at concentrations above its critical micellar concentration (CMC), i.e., 0.021% (w/v) (39). As in our experiments, the dose of Solutol[®] HS15 was about 860 mg/kg, and considering a blood volume of 1.7 mL/0.020 kg (22) and a Solutol[®] HS15 blood half-life in mice of 1.7 h (based on ¹⁴C-PEG analysis) (40), Solutol[®] HS15 blood concentrations were likely to be above CMC immediately after administration [estimated blood concentration: around 7.1 mg/mL (0.71%)] and over an extended period of time in blood. However, Solutol[®] HS15 is a highly complex mixture of polyethyleneglycol 660 (about 30%) and of polyethyleneglycol 660 mono- and diesters of 12-hydroxystearate (about 70%) with a small portion of the 12-hydroxy groups etherified with polyethyleneglycol (BASF Technical Bulletin, 2004). Such a chemical complexity, further increased by the polydispersity of the polyethyleneglycol moieties, makes structure/function analysis difficult (41). Its major components, polyethyleneglycol 660 esters of 12-hydroxystearic acid, were shown to display negligible multidrug resistance reversion activity compared with Solutol[®] HS15 itself (41). The minor components, polyethyleneglycol stearic or oleic ester derivatives, in particular diesters, were found to be efficient P-gp inhibitors *in vitro* (19,41,42). Previous *in vivo* studies aiming at evaluating the effect of Solutol[®] HS15, alone, on pharmacokinetics of intravenously administered drugs reported contradictory results (43,44). An alteration of the pharmacokinetic parameters in Wistar rats was observed for colchicin (43), but not for midazolam (44). The component(s) of Solutol[®] HS15 that presented P-gp inhibiting properties *in vitro* may therefore be of limited efficiency *in vivo* when administered alone or when included into LNC formulations.

Except in the case of liver where the increase in liver/plasma ratios may be attributed, at least in part, to the LNC early accumulation in liver (17), one has to consider mechanisms, alternative to a P-gp inhibition by LNC components, to account for the higher indinavir distribution into brain, testes, heart, and kidneys, when indinavir was administered as LNC formulation to both mouse substrains. LNC have a relatively long half disappearance time in blood (45 min) attributed to the presence of polyethyleneglycol chains at their surface (17). This prolonged circulation time in the

blood compartment may favor passive diffusion of LNC (38 ± 0.1 nm in diameter) into heart and kidney tissues, thus contributing to an increased indinavir uptake by these organs. LNC passive diffusion into brain and testes was excluded, because these organs are isolated from the blood compartment by a tight physiological barrier. In a previous study, LNC were indeed reported not to accumulate in brain (17). The disruption of blood-brain or blood testis barriers induced by the LNC formulation was also unlikely. In an *in situ* rat brain perfusion model, Lockman *et al.* (45) showed that cationic or anionic lipid nanoparticles did induce BBB disruption, but not neutral nanoparticles. As for chemical nature relating to the latter, LNC used in this study were reported to possess a slightly electronegative surface that is probably neutralized by positive ions present in blood (46). They, therefore, may have little impact on BBB permeability after intravenous administration. However, some LNC components, which includes Solutol[®] HS15, were shown to alter the cell membrane fluidity (47) and/or inhibit, at least in part, one of other efflux pumps involved in indinavir excretion, such as *mrp2* (36). One or both of the mechanisms may thus contribute in improving indinavir tissue distribution.

CONCLUSIONS

Results confirmed that P-gp governs, at least in part, the penetration of indinavir into tissues isolated by blood-tissue barriers. Furthermore, compared to Ind-Sol, LNC formulation increased the indinavir distribution not only into brain and testes, but also in heart, liver, and kidneys. The effect of LNC formulation probably involved mechanisms other than, or additional to, P-gp inhibition.

ACKNOWLEDGMENT

We are grateful for the excellent technical assistance of Mrs. Isabelle Lamarche.

REFERENCES

1. J. S. Lewis, C. M. Terriff, D. R. Coulston, and M. W. Garrison. Protease inhibitors: a therapeutic breakthrough for the treatment of patients with human immunodeficiency virus. *Clin. Ther.* **19**:187-214 (1997).
2. R. J. Pomerantz. Reservoirs of human immunodeficiency virus type 1: the main obstacles to viral eradication. *Clin. Infect. Dis.* **34**:91-97 (2002).
3. T. W. Chun and A. S. Fauci. Latent reservoirs of HIV: obstacles to the eradication of virus. *Proc. Natl. Acad. Sci. USA* **96**:10958-10961 (1999).
4. D. L. Kolson, E. Lavi, and F. Gonzalez-Scarano. The effects of human immunodeficiency virus in the central nervous system. *Adv. Virus Res.* **50**:1-47 (1998).
5. H. Zhang, G. Dornadula, M. Beaumont, L. J. Livornese, B. Van Uitert, K. Henning, and R. J. Pomerantz. Human immunodeficiency virus type 1 in the semen of men receiving highly active antiretroviral therapy. *N. Engl. J. Med.* **339**:1803-1809 (1998).
6. T. B. Kepler and A. S. Perelson. Drug concentration heterogeneity facilitates the evolution of drug resistance. *Proc. Natl. Acad. Sci. USA* **95**:11514-11519 (1998).
7. F. Thiebaut, T. Tsuruo, H. Hamada, M. M. Gottesman, I. Pastan, and M. C. Willingham. Cellular localization of the

- multidrug resistance gene product in normal human tissues. *Proc. Natl. Acad. Sci. USA* **84**:7735–7738 (1987).
8. C. Cordon-Cardo, J. P. O'Brien, D. Casals, L. Rittman-Grauer, J. L. Biedler, M. R. Melamed, and J. R. Bertino. Multidrug resistance gene (P-glycoprotein) is expressed by endothelial cells at blood brain barrier sites. *Proc. Natl. Acad. Sci. USA* **86**:695–698 (1989).
 9. E. C. de Lange. Potential role of ABC transporters as a detoxification system at the blood-CSF barrier. *Adv. Drug. Deliv. Rev.* **56**:1793–1809 (1989).
 10. N. Melaine, M. O. Lienard, I. Dorval, C. Le Goascogne, H. Lejeune, and B. Jegou. Multidrug resistance genes and P-glycoprotein in the testis of the rat, mouse, guinea pig and human. *Biol. Reprod.* **67**:1699–1707 (2002).
 11. R. B. Kim, M. F. Fromm, C. Wandel, A. J. Wood, D. M. Roden, and G. R. Wilkinson. The drug transporter P-glycoprotein limits oral absorption and brain entry of HIV protease inhibitors. *J. Clin. Invest.* **101**:289–294 (1998).
 12. E. F. Choo, B. Leake, C. Wandel, H. Imamura, A. J. Wood, G. R. Wilkinson, and R. B. Kim. Pharmacological inhibition of P-glycoprotein transport enhances the distribution of HIV-1 protease inhibitors into brain and testes. *Drug Metab. Dispos.* **28**:655–660 (2000).
 13. J. H. Lin. How significant is the role of P-glycoprotein in drug absorption and brain uptake? *Drugs Today (Barc.)* **40**:5–22 (2004).
 14. A. R. Bender, H. von Briesen, J. Kreuter, I. B. Duncan, and H. Rubsamens-Waigmann. Efficiency of nanoparticles as a carrier system for antiviral agents in human immunodeficiency virus-infected human monocytes/macrophages *in vitro*. *Antimicrob. Agents Chemother.* **40**:1467–1471 (1996).
 15. J. F. Gagne, A. Desormeaux, S. Perron, M. J. Tremblay, and M. G. Bergeron. Targeted delivery of indinavir to HIV-1 primary reservoirs with immunoliposomes. *Biochim. Biophys. Acta* **1558**:198–210 (2002).
 16. B. Heurtault, P. Saulnier, B. Pech, J. E. Proust, J. Richard, J.P. Benoit. A novel phase inversion-based process for the preparation of lipidic nanocarriers, 2000. Patent FR 0002688.
 17. A. Cahouet, B. Denizot, F. Hindre, C. Passirani, B. Heurtault, M. Moreau, J. Le Jeune, and J. P. Benoit. Biodistribution of dual radiolabeled lipidic nanocapsules in the rat using scintigraphy and gamma counting. *Int. J. Pharm.* **242**:367–371 (2002).
 18. J. S. Coon, W. Knudson, K. Clodfelter, B. Lu, and R. S. Weinstein. Solutol HS 15, non toxic polyethylene esters of 12-hydroxystearic acid reverses multidrug resistance. *Cancer Res.* **51**:897–902 (1991).
 19. L. E. Buckingham, M. Balasubramanian, A. R. Safa, H. Shah, P. Komarov, R. M. Emanuele, and J. S. Coon. Reversal of multidrug resistance *in vitro* by fatty acid-PEG-fatty acid diester. *Int. J. Cancer* **65**:74–79 (1996).
 20. R. C. Bravo Gonzalez, J. Huwyler, F. Boess, I. Walter, and B. Bittner. *In vitro* investigation on the impact of the surface-active excipients Cremophor EL, Tween 80 and Solutol HS 15 on the metabolism of midazolam. *Biopharm. Drug Dispos.* **25**:37–49 (2004).
 21. L. Y. Li, G. L. Amidon, J. S. Kim, T. Heimbach, F. Kesisoglou, J. T. Topliss, and D. Fleisher. Intestinal metabolism promotes regional differences in apical uptake of indinavir: coupled effect of P-glycoprotein and cytochrome P450 3A on indinavir membrane permeability in rat. *J. Pharmacol. Exp. Ther.* **301**:586–593 (2002).
 22. F. L. S. Tse. Pharmacokinetics in drug discovery and development: nonclinical studies. In P. G. Welling and F. L. S. Tse (eds.), *Pharmacokinetics: Regulatory, Industrial, Academic Perspectives*, 2nd ed., Marcel Dekker, New York, 1995, pp. 281–334.
 23. E. Y. Wu, J. M. Wilkinson, D. G. Naret, V. L. Daniels, L. J. Williams, D. A. Khalil, and B. V. Shetty. High-performance liquid chromatographic method for the determination of nelfinavir, a novel HIV-1 protease inhibitor, in human plasma. *J. Chromatogr. B Biomed. Sci. Appl.* **695**:373–380 (1997).
 24. R. P. van Heeswijk, R. M. Hoetelmans, R. Harms, P. L. Meenhorst, J. W. Mulder, J. M. Lange, and J. H. Beijnen. Simultaneous quantitative determination of the HIV protease inhibitors amprenavir, indinavir, nelfinavir, ritonavir and saquinavir in human plasma by ion-pair high-performance liquid chromatography with ultraviolet detection. *J. Chromatogr. B Biomed. Sci. Appl.* **719**:159–168 (1998).
 25. J. Chi, A. L. Jayewardene, J. A. Stone, T. Motoya, and F. T. Aweeka. Simultaneous determination of five HIV protease inhibitors nelfinavir, indinavir, ritonavir, saquinavir and amprenavir in human plasma by LC/MS/MS. *J. Pharm. Biomed. Anal.* **30**:675–684 (2002).
 26. J. M. Croop, M. Raymond, D. Haber, A. Devault, R. J. Arceci, P. Gros, and D. E. Housman. The three mouse multidrug resistance (mdr) genes are expressed in a tissue-specific manner in normal mouse tissues. *Mol. Cell Biol.* **9**:1346–1350 (1989).
 27. T. R. Pippert and D. R. Umbenhauer. The subpopulation of CF-1 mice deficient in P-glycoprotein contains a murine retroviral insertion in the mdr1a gene. *J. Biochem. Mol. Toxicol.* **15**:83–89 (2001).
 28. E. G. Schuetz, D. R. Umbenhauer, K. Yasuda, C. Brimer, L. Nguyen, M. V. Relling, J. D. Schuetz, and A. H. Schinckel. Altered expression of hepatic cytochromes P-450 in mice deficient in one or more mdr1 genes. *Mol. Pharmacol.* **57**:188–197 (2000).
 29. G. R. Lankas, M. E. Cartwright, and D. Umbenhauer. P-glycoprotein deficiency in a subpopulation of CF-1 mice enhances ivermectin-induced neurotoxicity. *Toxicol. Appl. Pharmacol.* **143**:357–365 (1997).
 30. J. A. Bush and G. Li. Regulation of the mdr1 isoforms in a p53-deficient mouse model. *Carcinogenesis* **23**:1603–1607 (2002).
 31. N. Mizuno, T. Niwa, Y. Yotsumoto, and Y. Sugiyama. Impact of drug transporter studies on drug discovery and development. *Pharmacol. Rev.* **55**:425–461 (2003).
 32. A. H. Schinckel, U. Mayer, E. Wagenaar, C. A. Mol, L. van Deemter, J. J. Smit, M. A. van der Valk, A. C. Voordouw, H. Spits, O. van Tellingen, J. M. Zijlmans, W. E. Fibbe, and P. Borst. Normal viability and altered pharmacokinetics in mice lacking mdr1-type (drug-transporting) P-glycoproteins. *Proc. Natl. Acad. Sci. USA* **94**:4028–4033 (1997).
 33. J. A. Holash, S. I. Harik, G. Perry, and P. A. Stewart. Barrier properties of testis microvessels. *Proc. Natl. Acad. Sci. USA* **90**:11069–11073 (1993).
 34. J. van Asperen, O. van Tellingen, F. Tijssen, A. H. Schinckel, and J. H. Beijnen. Increased accumulation of doxorubicin and doxorubicinol in cardiac tissue of mice lacking *mdr1a* P-glycoprotein. *Br. J. Cancer* **79**:108–113 (1999).
 35. J. Jodoin, M. Demeule, L. Fenart, R. Cecchelli, S. Farmer, K. J. Linton, C. F. Higgins, and R. Beliveau. P-glycoprotein in blood-brain barrier endothelial cells: interaction and oligomerization with caveolins. *J. Neurochem.* **87**:1010–1023 (2003).
 36. M. T. Huisman, J. W. Smit, K. M. Crommentuyn, N. Zelcer, H. R. Wiltshire, J. H. Beijnen, and A. H. Schinckel. Multidrug resistance protein 2 (MRP2) transports HIV protease inhibitors and transport can be enhanced by other drugs. *AIDS* **16**:2295–2301 (2002).
 37. A. Rosati, S. Maniori, G. Decorti, L. Candussio, T. Giralaldi, and F. Bartoli. Physiological regulation of P-glycoprotein MRP1, MRP2 and cytochrome P 450 3A2 during rat ontogeny. *Dev. Growth Differ.* **45**:377–387 (2003).
 38. A. S. Chong, P. N. Markham, H. M. Gebel, S. D. Bines, and J. S. Coon. Diverse multidrug-resistance-modification agents inhibit cytolytic activity of natural killer cells. *Cancer Immunol. Immunother.* **36**:133–139 (1993).
 39. K. Buszello, S. Harnisch, R. H. Muller, and B. W. Muller. The influence of alkali fatty acids on the properties and the stability of parenteral O/W emulsions modified with Solutol HS15. *Eur. J. Pharm. Biopharm.* **49**:143–149 (2000).
 40. K. Woodburn, E. Sykes, and D. Kessel. Interactions of Solutol HS 15 and Cremophor EL with plasma lipoproteins. *Int. J. Biochem. Cell Biol.* **27**:693–699 (1995).
 41. L. E. Buckingham, M. Balasubramanian, R. M. Emanuele, K. E. Clodfelter, and J. S. Coon. Comparison of Solutol HS 15, Cremophor EL and novel ethoxylated fatty acid surfactants as multidrug resistance modification agents. *Int. J. Cancer* **62**:436–442 (1995).
 42. P. G. Komarov, A. A. Shtil, L. E. Buckingham, M. Balasubramanian, O. Piraner, R. M. Emanuele, I. B. Roninson,

- and J. S. Coon. Inhibition of cytarabine-induced MDR1 (P-glycoprotein) gene activation in human tumor cells by fatty acid-polyethylene glycol-fatty acid diesters, novel inhibitors of P-glycoprotein function. *Int. J. Cancer* **68**:245-250 (1996).
43. B. Bittner, R. C. Gonzalez, I. Walter, M. Kapps, and J. Huwyler. Impact of Solutol HS 15 on the pharmacokinetic behaviour of colchicine upon intravenous administration to male Wistar rats. *Biopharm. Drug Dispos.* **24**:173-181 (2003).
44. B. Bittner, R. C. Gonzalez, H. Isel, and C. Flament. Impact of Solutol HS 15 on the pharmacokinetic behavior of midazolam upon intravenous administration to male Wistar rats. *Eur. J. Pharm. Biopharm.* **56**:143-146 (2003).
45. P. R. Lockman, J. Koziara, K. E. Roder, J. Paulson, T. J. Abbruscato, R. J. Mumper, and D. D. Allen. *In vivo* and *in vitro* assessment of baseline blood-brain barrier parameters in the presence of novel nanoparticles. *Pharm. Res.* **56**:705-713 (2003).
46. A. Vonarbourg, P. Saulnier, C. Passirani, and J. P. Benoit. Electrokinetic properties of noncharged lipid nanocapsules: influence of the dipolar distribution at the interface. *Electrophoresis* **26**:2066-2075 (2005).
47. P. K. Dudeja, K. M. Anderson, J. S. Harris, L. Buckingham, and J. S. Coon. Reversal of multidrug resistance phenotype by surfactants: relationship to membrane lipid fluidity. *Arch Biochem. Biophys.* **319**:309-315 (1995).